

A comparative theoretical study of the hydride transfer mechanisms during LiAlH₄ and LiBH₄ reductions

メタデータ	言語: eng 出版者: 公開日: 2017-12-05 キーワード (Ja): キーワード (En): 作成者: メールアドレス: 所属:
URL	https://doi.org/10.24517/00010817

This work is licensed under a Creative Commons Attribution-NonCommercial-ShareAlike 3.0 International License.



A comparative theoretical study of the hydride transfer mechanisms during LiAlH₄ and LiBH₄ reductions

Yuta Hori*, Tomonori Ida and Motohiro Mizuno

Chemistry Course, Division of Material Chemistry, Graduate School of Natural Science and Technology, Kanazawa University, Kanazawa 920-1192

E-mail: yu.hori59@gmail.com Tel:+81-76-264-5924 Fax: +81-76-264-5742

Abstract

This work examined the hydride transfer processes during the reduction of formaldehyde by LiAlH₄ or LiBH₄, including investigations of the geometries, solvent effects and charge transfer processes along the reaction coordinate, using density functional theory (DFT). The energy and geometry results demonstrate that the transition state (TS) structure for the LiAlH₄-formaldehyde complex is reactant-like, while the structure generated by LiBH₄ has a product-like geometry, consistent with the Hammond postulate. From a charge density analysis, we also found that both complexes undergo the same essential hydride transfer mechanism, which consists of: (1) single electron transfer to the carbonyl carbon, (2) formation of a bridge bond (X-H-C; X = Al or B) and (3) hydrogen transfer driven by electron transfer. Subsequently, in a fourth step, a single electron flows through the X-H-C bond during transfer of the hydrogen, such that hydrogen atom or proton-coupled electron transfer occurs. In both systems, the presence of tetrahydrofuran as a solvent affects the structure and energy values during the reaction, but not the charge transfer characteristics. We propose that the rate-determining steps during hydride transfer when employing LiAlH₄ and LiBH₄ are one electron transfer to the carbonyl carbon and B-H bond dissociation, respectively.

1. Introduction

Reductions involving hydride transfers are some of the most important chemical reactions in biochemistry and organic chemistry [1-3]. As an example, NADPH [4], FADH₂ [5], tetrahydrofolate [6] and ascorbic acid [7], all of which play vital roles in biological redox systems, are naturally-produced organic hydride donors. The reductions of ketones [8], aldehydes [9], alkenes [10], alkyl halides [11] and imines [12] are also well-known reactions involving hydride transfers. As such, there is considerable interest among researchers regarding the design and synthesis of new organic

compounds via hydride reductions.

Hydride transfer is a key process in hydride reduction and so, to elucidate the associated reaction mechanism, it is important to understand the hydride reduction mechanism. In previous works, the hydride transfer mechanisms in many biological and organic reduction systems were investigated using either experimental or theoretical approaches [13-24]. Although these mechanisms have not yet been fully explained due to the variety of possible pathways involving the overall transfer of two electrons and one proton, the following hydride transfer mechanisms have been proposed: (1) direct transfer of a hydride ion (H^-) in a single step, (2) two-step transfer of an electron before or after the transfer of a hydrogen atom and (3) transfer of two electrons and one proton in three separate steps. Several experimental studies have provided evidence for the single-step mechanism [25-28], although the multi-step mechanism has also been suggested [19,28,29]. Therefore, although the hydride transfer mechanism has been researched over a significant time period, there is little agreement as to the detailed reaction steps.

Theoretical studies aimed at understanding the hydride transfer mechanism have also been conducted, focusing on the effects of the charge density, ionization potential and proton affinity of the reactant and transition state [13-18,21,23,24]. However, as far as we know, there are no reports of detailed charge density analysis along the reaction coordinates during hydride transfer, although it requires complete information regarding the dynamics of the mechanism. Furthermore, hydride transfer process would be strongly affected by various solvent species, because the process involves the transfer of two electrons and it is well known that the dynamics and kinetics of such transfers are affected by the solvent.

In the present study, we focused on a hydride transfer system in which formaldehyde (CH_2O) acts as the hydride acceptor and lithium aluminum hydride (LiAlH_4) or lithium borohydride (LiBH_4) acts as the hydride donor. LiAlH_4 and LiBH_4 have both been widely used in organic syntheses as reducing agents, although LiAlH_4 is more powerful than LiBH_4 owing to the weaker Al-H bond compared to the B-H bond [3]. A suggested hydride reduction mechanism using these reducing agents is shown in Scheme 1. The reaction path, geometries and energies of the complexes and transition state (TS) structures in these reactions have been previously investigated using many experimental and theoretical approaches [30-39]. These studies have identified the importance of the association of the lithium cation with the carbonyl oxygen during reduction by LiAlH_4 or LiBH_4 . In addition, it was found that this structures remained in solvent by Car-Prrinello molecular dynamics simulations about a solution of NaBH_4 in

liquid methanol [39]. Both carbonyl carbon-14 and deuterium isotope studies during the reduction of benzophenone with NaBH_4 , LiBH_4 and LiAlH_4 have shown that changing the metal atom from Al to B shifts the transition state geometry from reactant-like to central, and that varying the solvent can generate a product-like TS [39]. Furthermore it is necessary to study the behavior of hydrides in terms of their geometries, energies and charge densities to fully understand the hydride transfer mechanism. Tetrahydrofuran (THF) is often used as the solvent during laboratory-scale hydride reduction with LiAlH_4 and LiBH_4 . Therefore, we also study the behavior of hydrides for polarizability of THF.

In this work, we calculated optimized geometries for the reactant, transition and product states both under vacuum and in THF, focusing on changes in the dynamics of transferring the H atom as well as the charge density along the reaction coordinate. The reduction of CH_2O using either LiAlH_4 or LiBH_4 was assessed. To accomplish this, we calculated intrinsic reaction coordinate (IRC) both under vacuum and in THF for these reaction systems, and analyzed the molecular and electronic structures along the IRC using density functional theory (DFT). Based on the results, we deduced the essential hydride transfer mechanism by clarifying the charge transfer behavior along the IRC. Herein we discuss the differences in the reaction process observed when employing either LiAlH_4 or LiBH_4 as reagents by comparing the two systems in terms of their geometries, energies and charge densities.

2. Computational Details

In the present study, we focused on the hydride transfer system in which CH_2O is the hydride acceptor and LiAlH_4 or LiBH_4 is the hydride donor. All DFT calculations were conducted at the CAM-B3LYP/Aug-cc-pVTZ level with the Gaussian 09 software package [40]. CAM-B3LYP is a long-range corrected version of B3LYP that employs the Coulomb-attenuating method. Although the conventional B3LYP method is typically used to investigate charge density [47] and solvent effects [44], CAM-B3LYP improves upon B3LYP since the latter is unsuccessful in a number of important applications, such as when determining the polarizability of long chains, excitations of Rydberg states and especially charge transfer effects [41-43]. Using this approach, we calculated IRC to characterize the reaction path by determining the minimum energy reaction pathway from the optimized TS structure. The hydride transfer TS was optimized based on the results of previous studies [32, 38]. In addition, we calculated the energy of RS, TS, and PS using CCSD(T)/Aug-cc-pVTZ level for obtained above geometries to confirm the accuracy of CAM-B3LYP calculations. Although solvent molecules are interacted to the

solute molecules, the importance of the association of the lithium cation with the carbonyl oxygen during reduction by LiAlH_4 or LiBH_4 is recognized in the previous work [39]. Thus, in this work, we considered the polarizability of THF as the solvent effects. The solvent effects were evaluated using the self-consistent reaction field polarizable continuum model (SCRF/PCM) [44,45]. In previous work, the solvation free energies and dipole moments of organic molecules obtained using SCRF/PCM were found to be in good agreement with experimental data [44]. To investigate the hydride transfer process in detail, we estimated the rearrangement parameter (α) and charge density of the fragments involved in the hydride transfer process along the IRC. Here α denotes the extent of transfer of a H atom from the reactant to product structures, and is defined as:

$$\alpha \equiv \frac{\Delta R_{\text{X-H}}}{\Delta R_{\text{C-H}} + \Delta R_{\text{X-H}}} \quad (\text{X} = \text{Al, B}),$$

where $\Delta R_{\text{C-H}}$ is obtained by subtracting the length of the bond between the carbon and the transferring H atom from the C-H bond length in the methoxide ion (CH_3O^-) and $\Delta R_{\text{X-H}}$ is obtained by subtracting the length of the bond between the X atom and the transferring H atom from the X-H bond length in the XH_4^- reactant. A value of $\alpha = 0$ indicates that the structure at a given stage is close to the initial structure (that is, XH_4^-), while a value of $\alpha = 1$ corresponds to a structure more closely resembling that of the product (CH_3O^-). Charge density values were obtained by calculating the electrostatic potential fit (ESP) charges using the Merz-Killmann (MK) method. The charge distribution derived from ESP typically exhibits the best performance in both theoretical and experimental investigations [46-48], compared to data derived from the Mulliken, Hirshfeld and Natural Population Analysis schemes [49], and is also used for the analysis of chemical trends [50].

3. Results and Discussion

To investigate the role of the lithium cation (Li^+) during hydride reduction by LiAlH_4 and LiBH_4 , we first calculated the IRC for hydride transfers with and without Li^+ . The activation energy (ΔE_a) and the energy difference (ΔE) between the reactant state (RS) and product state (PS) were then estimated, where ΔE_a and ΔE were obtained by subtracting the energy of the TS from the RS and the energy of the PS from the RS based on the IRC results, respectively. Table 1 summarizes the ΔE_a and ΔE values for hydride transfer under vacuum. To confirm the accuracy of CAM-B3LYP

calculations, we also calculated the ΔE_a and ΔE values using CCSD(T) for obtained above geometries. The obtained ΔE_a and ΔE values were respectively 14.6 and -192 kJ/mol for LiAlH₄ system, while that values were 82.7 and -115 kJ/mol for LiBH₄ system, which were close agreement with the values using CAM-B3LYP (see Table 1). In the case of both reagents, these values indicate that ΔE_a is significantly decreased in the presence of Li⁺, while ΔE is not greatly changed. These results are consistent with those of previous work [31]. These data suggest that the lithium cation contributes to stabilization of the TS, and is an important factor promoting the hydride reduction.

Figure 1 shows the RS, TS and PS structures associated with hydride transfer via LiAlH₄ and LiBH₄-formaldehyde complexes under vacuum. The TSs were obtained by an optimization process, and the RS and PS were located along both sides of the IRC compared to the TS. The complex formation energies, obtained by subtracting the energies of formation of formaldehyde and LiAlH₄ or LiBH₄ from the RS energy, were determined to be -87.1 and -76.5 kJ/mol, respectively. These results indicate that formation of the complex (the RS), meaning the coordination of lithium to oxygen, occurs prior to transfer of the hydride to the carbonyl carbon [32]. With regard to the structures of the RS, TS and PS, no differences in bonding state were found between the LiAlH₄ and LiBH₄ complexes. In the RS and TS of both complexes, a lithium tridentate structure was identified, corresponding to the coordination of lithium to an oxygen and two hydrogens. The TS structures were found to be both six-centered cyclic forms, in which the C...H bond lengths generated when employing LiAlH₄ and LiBH₄ were 1.76 and 1.12 Å, respectively. Therefore the TS structure associated with LiAlH₄ reduction has a reactant-like geometry, whereas TS structure associated with LiBH₄ reduction is product-like. The PS obtained from both complexes has the same conformation, in which aluminum and boron are associated with oxygen, and the AlH₃ and BH₃ moieties are rotated to allow the coordination of lithium to one hydrogen, respectively. Furthermore, by comparing the ΔE_a and ΔE values for both complexes, we also found that the use of LiAlH₄ resulted in lower ΔE_a and ΔE compared to the results obtained with LiBH₄ [32,38], in agreement with the experimental observation [39] that the reducing power of LiBH₄ is less than that of LiAlH₄.

To examine the solvent effects on the hydride transfer, we perform IRC calculation including one explicit molecule of THF and under PCM for LiAlH₄ system as the same method under Vacuum. Since THF is well-known to complex lithium, in explicit THF molecule, TS is explored based on the configurations in Vacuum and interacted THF to the lithium. Figure 2, 3(a) and Table 2 show the structures of the RS, TS, PS, and relative energies (ΔE_a and ΔE) in explicit model and PCM for LiAlH₄ system. These

results indicate that RS, TS, and PS structures have similar conformations for explicit model and PCM of THF. Also, relative energies are close values for these two models. In calculations of the explicit model with THF molecules, various geometries are expected to be obtained by the relative positions, orientations, and number of THF molecules. In this study, we focus on a local dynamics of hydride transfer, not the relationship between LiAlH₄ or LiBH₄ systems and explicit THF in detail. So, the PCM calculation as the solvent effects was employed in following.

Table 3 shows the total energies of the RS, TS and PS as well as the ΔE_a and ΔE values both under vacuum and in THF. In the case of both reagents, the total energies of the RS, TS and PS are all reduced when performing the reaction in THF, as are ΔE_a and ΔE . These results suggest that the TS and PS are more highly stabilized than the RS in the presence of THF.

Figure 3 presents the structures of the RS, TS and PS in THF. For both complexes, different TS structures were obtained with and without the solvent. When using LiAlH₄, the TS structure contains bidentate lithium, in which lithium is coordinated to an oxygen and a hydrogen, while a tridentate structure appears under vacuum. In contrast, for the LiBH₄ system, a linear structure with a Li-O-C bond was identified. It is evident that these structures involve more charge separation, and thus is more highly stabilized by the presence of a solvent, in agreement with the results of previous work [32,36]. Especially, when using LiBH₄, the solvent thus has a more significant effect on the activation energy compared with the LiAlH₄ system. This stabilization could be related to the conformational changes induced in the RS and TS by the solvent. The RS structures for both complexes have similar conformations to the TS structures in THF, while the PS structures are significantly different from the TS due to structural relaxation, as was also observed under vacuum.

From the above, we confirmed that the calculated energies and geometries of the RS, TS and PS were consistent with those determined in previous studies. We next investigated changes in the structure and energy during the hydride transfer process in detail, using the rearrangement parameter; α , and the relative energies of the RS along the IRC. From this, the H atom transfer mechanism during the hydride transfer process was elucidated. Herein, the transferred H atom is denoted by 'H', which is not distinguished from the hydride ion (H⁻), hydrogen atom (H) and proton (H⁺). Figures 4 and 5 summarize the values of α and the relative energies of the RS along the IRC for LiAlH₄ and LiBH₄-formaldehyde complexes under vacuum and in THF. From these figures it is evident that α is not varied by the presence or absence of THF for the LiAlH₄ system, and remains at 0 up to the point at which the TS appears. These data

indicate that the TS exists as a reactant-like structure in this chemical reaction. Once the 'H' has completely transferred to the carbonyl carbon, the energy decreases drastically and the structure changes to the PS due to structural relaxation, moving from IRC = 7 to 15.

Conversely, in the case of the LiBH₄ system, different values of α were found depending on the presence of the solvent. With THF, the α value at the RS has already exceeded 0.5, signifying that the 'H' transfer is more than halfway complete. The change in α at the RS can be explained by the conformational changes resulting from charge responses to the solvent effect. Thus, the carbonyl carbon more closely approaches the boron in the RS in THF because a Li-O-C bond is generated by the solvent effect. In the case of both vacuum and THF conditions, the 'H' transfer to the carbonyl carbon initiates prior to passing the TS, such that the transfer is complete just before formation of the TS (IRC = 0), corresponding to a product-like structure. When using LiBH₄, once the 'H' has completely transferred to the carbonyl carbon, as is also the case with LiAlH₄, the energy has decreased and the structure changes to the PS due to structural relaxation.

Comparing the mechanisms of both complexes moving from the RS to TS, we determined that the 'H' transfer in the case of LiAlH₄ begins in the vicinity of the TS, and thus can be considered an early barrier reaction, while the 'H' transfer with LiBH₄ had finished in the vicinity of the TS, indicating a late barrier reaction. These results are consistent with the Hammond postulate [51] based on the fact that a TS structure having a low activation energy is reactant-like, while a structure with a high activation energy is product-like. The data indicate that the rate determine step in the hydride transfer is different when using LiAlH₄ compared to the use of LiBH₄.

Finally, to clarify the charge transfer dynamics, we calculated the changes in charge density during the hydride transfer process along the IRC. Charge densities were obtained by considering four fragments: CH₂O, AlH₃ or BH₃, 'H' and Li⁺. Figures 6 and 7 show the charge density results obtained for the LiAlH₄ and LiBH₄-formaldehyde complexes under vacuum and in THF, respectively. The charge density for Li⁺ was not plotted in these figures because, for both LiAlH₄ and LiBH₄, the Li⁺ charge was invariant over the course of the reaction. In either system, the negative charge of the CH₂O fragment is seen to increase, while that of the AlH₃ or BH₃ decreases during 'H' transfer. These results indicate electron transfer from the AlH₃ or BH₃ fragment to CH₂O during the 'H' transfer.

We subsequently focused on the charge density of the LiAlH₄ system under vacuum, because the solvent effect was not observed in the case of the charge density

for this system. The charge transfer parameter for the CH_2O fragment was estimated so as to clearly understand the relationship between the 'H' and electron transfers. This parameter was calculated by setting the charges at the RS and PS to 0 and 1, respectively. Figure 8 summarizes the variations in the rearrangement and charge transfer parameter with IRC. From Figure 8(a), it can be seen that the charge transfer parameter increases prior to the 'H' transfer, suggesting that a one electron transfer occurs before the 'H' transfer. Figure 6(a) shows that the negative charge of the CH_2O fragment increases during the 'H' transfer, while the negative charge of the transferring 'H' gradually decreases. Therefore, the 'H' transfers to the carbonyl carbon along with the electron transfer. We also calculated the bond order of the Al-H and C-H bonds to investigate the behavior of the chemical bond during hydride transfer. The calculated bond orders for Al-H and C-H were 0.73 and 0.00 at the RS, but 0.57 and 0.28 at the TS, respectively. These results indicate that an Al-H-C bond is formed as the one electron transfer takes place prior to the 'H' transfer. In summary, hydride transfer using LiAlH_4 proceeds as follows: (1) a one electron transfer to the carbonyl carbon occurs, (2) a bridge bond (the Al-H-C bond) forms, (3) the 'H' transfer begins, with electron transfer as the driving force, and finally (4) a single electron subsequently moves gradually toward the carbonyl carbon through the Al-H-C bond while the 'H' transfers.

In the case of LiBH_4 , a solvent effect on the charge density was observed. The changes in charge could be explained by conformational changes of the RS and TS structures by solvent effects. We estimated the charge transfer parameter in the same manner as for the LiAlH_4 system. Figure 8(b) shows that the negative charge of the CH_2O fragment increases before the 'H' transfer, which is the same result as obtained with LiAlH_4 . The bond order calculated for B-H and C-H were 0.78 and 0.00 at the RS, and 0.71 and 0.26 at IRC = 5, respectively. From these results, we found that a B-H-C bond was formed via one electron transfer in advance of the 'H' transfer, just as with LiAlH_4 . In summary, we found that the essential mechanism of the hydride transfer using LiBH_4 was the same as that when using LiAlH_4 .

From these charge density analyses, we ascertained that the relationship between charge transfer and hydride transfer is the same when employing either LiAlH_4 or LiBH_4 . However, the TS structures in both systems are different, representing reactant-like and product-like structures, respectively. By comparing the TS structures of both systems, we also found that the rate-determining steps in the hydride transfer are one electron transfer to the carbonyl carbon for the LiAlH_4 system, and B-H bond dissociation for the LiBH_4 system. The presence of THF affects the structure and energy values throughout the reaction by influencing charge separation, although the hydride

transfer and the charge are not affected by the solvent.

4. Conclusion

We studied the differences in the geometry of the reactant, transition and product states under vacuum and in THF as well as the dynamic changes associated with the transfer of the H atom and the charge density along the reaction coordinate for the reduction of formaldehyde by LiAlH₄ or LiBH₄, using DFT calculations. We obtained information about the hydride transfer mechanism that allowed us to investigate the behavior of the hydride and the charge density along the IRC. The resulting data indicated that Li⁺ contributes to the stabilization of the TS, and this effect is more pronounced in the presence of a solvent. The TS structure associated with the LiAlH₄-formaldehyde complex is reactant-like, while the LiBH₄ structure is product-like. These results are consistent with the Hammond postulate, because the activation energy for the LiAlH₄ system is lower than that for LiBH₄. Although these results are also in agreement with various previous reports, the work presented herein goes further so as to allow a detailed understanding of the hydride transfer mechanism based on our computational results for the geometries, energies and charge densities and comparison of both systems.

The essential mechanism of the hydride transfer is the same for both reducing agents, and may be summarized as follows: (1) one electron transfer to the carbonyl carbon, (2) formation of a bridge bond (X-H-C bond; X = Al or B), (3) initiation of 'H' transfer driven by electron transfer and (4) one electron flow through the X-H-C bond in conjunction with transfer of the 'H', during which the hydrogen atom or proton-coupled electron transfer occurs. The presence of a solvent affects the structure and energy values through charge separation, but has no effect on the hydride transfer and charge. Finally, this study suggests that the rate-determining steps in the hydride transfer when employing LiAlH₄ and LiBH₄ are one electron transfer to the carbonyl carbon and B-H bond dissociation, respectively.

References

- [1] N. C. Deno, H. J. Peterson, G. S. Saines, THE HYDRIDE-TRANSFER REACTION, *Chem. Rev.* 60, (1960), 7-14.
- [2] C. Ian, F. Watt, Hydride Shifts and Transfers, *Adv. Phys. Org. Chem.* 24, (1988), 57-112.

- [3] J. Clayden, N. Greeves, S. Warren, P. Wothers, *Organic Chemistry*, Oxford University Press, 2001.
- [4] Y. Murakami, J.-I. Kikuchi, Y. Hisaeda, O. Hayashida, *Artificial Enzymes*, *Chem. Rev.* 96, (1996), 721-758.
- [5] P. F. Fitzpatrick, *Substrate Dehydrogenation by Flavoproteins*, *Acc. Chem. Res.* 34, (2001), 299-307.
- [6] B. Y. Hong, M. Haddad, F. Maley, J. H. Jensen, A. Kohen, *Hydride Transfer versus Hydrogen Radical Transfer in Thymidylate*, *J. Am. Chem. Soc.* 128, (2006), 5636-5637.
- [7] P. Neta, *Reactions of hydrogen atoms in aqueous solutions*, *Chem. Rev.* 72, (1972), 533-543.
- [8] J.-S. Song, D. J. Szalda, R. M. Bullock, *Alcohol Complexes of Tungsten Prepared by Ionic Hydrogenations of Ketones*, *Organometallics*, 20, (2001), 3337-3346.
- [9] P. L. Gaus, S. C. Kao, K. Youngdahl, M. Y. Darensbourg, *Anionic group 6 transition-metal carbonyl hydrides as reducing agents. Ketones, aldehydes, and epoxides*, *J. Am. Chem. Soc.* 107, (1985), 2428-2434.
- [10] R. M. Bullock, J.-S. Song, *Ionic Hydrogenations of Hindered Olefins at Low Temperature. Hydride Transfer Reactions of Transition Metal Hydrides*, *J. Am. Chem. Soc.* 116, (1994), 8602-8612.
- [11] S. C. Kao, C. T. Spillett, C. Ash, R. Lusk, Y. K. Park, M. Y. Darensbourg, *Relative reactivity and mechanistic studies of the hydride-transfer reagents $\text{HM}(\text{CO})_4\text{L}-(\text{M}=\text{Cr}, \text{W}; \text{L}=\text{CO}, \text{PR}_3)$* , *Organometallics* 4, (1985), 83-91.
- [12] M. P. Magee, J. R. Norton, *Stoichiometric, Catalytic, and Enantioface-Selective Hydrogenation of C=N Bonds by an Ionic Mechanism*, *J. Am. Chem. Soc.* 123, (2001), 1778-1779.
- [13] O. Tapia, J. Andres, J. M. Aullo, C.-I. Bränden, *Electronic aspects of the hydride transfer mechanism. Ab initio analytical gradient studies of the cyclopropenyl-cation/lithium hydride model reactant system*, *J. Chem. Phys.* 83, (1985), 4673- 4682.
- [14] O. Tapia, J. Andres, J. M. Aullo, R. Cardenas, *ELECTRONIC ASPECTS OF THE HYDRIDE TRANSFER MECHANISM*, *J. Mol. Struct., Theochem* 167, (1988), 395-412.
- [15] J. Mestres, A. Lledo's, M. Duran, J. Bertra'n, *Analysis of the hydride transfer in the $[\text{CH}_3\text{-H-CH}_3]^+$ system in terms of valence bond structures*, *J. Mol. Struct., Theochem* 260, (1992), 259-272.

- [16] J. Mestres, M. Duran, J. Bertrán, Analysis of the hydride transfer in the $[\text{CH}_3\text{-H-CH}_3]^+$ system, *Theor. Chim. Acta* 88, (1994), 325–338.
- [17] J. Mestres, M. Duran, J. Bertrán, Characterization of the Transition State for the Hydride Transfer in a Model of the Flavoprotein Reductase Class of Enzymes, *Bioorganic Chemistry* 80, (1996), 69–80.
- [18] X. Fradera, M. Duran, J. Mestres, Comparative electronic analysis between hydrogen transfers in the $\text{CH}_4/\text{CH}_3^+$, $\text{CH}_4/\text{CH}_3^\bullet$, and $\text{CH}_4/\text{CH}_3^-$ systems: on the electronic nature of the hydrogen (H^- , H^\bullet , H^+) being transferred. II. Analysis of electron-pair interactions from intracule and extracule densities, *Can. J. Chem.* 78, (2000), 328–337.
- [19] X. Q. Zhu, Y. Liu, B. J. Zhao, J. P. Cheng, An Old but Simple and Efficient Method to Elucidate the Oxidation Mechanism of NAD(P)H Model 1-Aryl-1,4-dihydronicotinamides by Cations 2-Methyl-5-nitroisoquinolium, Tropylium, and Xanthylium in Aqueous solution, *J. Org. Chem.* 66, (2001), 370–375.
- [20] J. Gębicki, A. Marcinek, J. Zielonka, Transient species in the stepwise interconversion of NADH and NAD^+ , *Acc. Chem. Res.* 37, (2004), 379–386.
- [21] A. N. Pankratov, B. I. Drevko, An approach to quantum chemical consideration of "hydride" transfer reactions, *J. Serb. Chem. Soc.* 69, (2004), 431–439.
- [22] H. Buck, Charge at the Migrating Hydrogen in the Transition State of Hydride Transfer Reactions From CH Groups to Hydride Acceptors. Dynamics of the Redox-Couple NADH-NAD^+ , *Int. J. Quant. Chem.* 101, (2005), 389–395.
- [23] A. N. Pankratov, B. I. Drevko, QUANTUM-CHEMICAL STUDY OF "HYDRIDE" MOBILITY IN THE MOLECULES OF CHALCOGENOPYRANS, *Chemistry of Heterocyclic Compounds*, 41, (2005), 1105–1111.
- [24] S. Khanna, D. Kaur, R. Kaur, The saturated five-membered heterocyclic molecules as organic hydride donors: a computational study, *J. Phys. Org. Chem.* 27, (2014), 747–755.
- [25] M. F. Powell, J. C. Wu, T. C. Bruice, Ferricyanide oxidation of dihydropyridines and analogs, *J. Am. Chem. Soc.* 106, (1984), 3850–3856.
- [26] L. L. Miller, J. R. Valentine, On the Electron-Proton-Electron Mechanism for 1-Benzyl-1,4-dihydronicotinamide Oxidations, *J. Am. Chem. Soc.* 110, (1988), 3982–3989.
- [27] M. F. Powell, T. C. Bruice, Hydride vs. Electron Transfer in the Reduction of Flavin and Flavin Radical by 1,4-Dihydropyridines, *J. Am. Chem. Soc.* 105, (1983), 1014–1021.

- [28] J.-P. Cheng, Y. Lu, X. Zhu, L. Mu, Energetics of Multistep versus One-step Hydride Transfer Reactions of Reduced Nicotinamide Adenine Dinucleotide (NADH) Models with Organic Cations and *p*-Quinones, *J. Org. Chem.* 63, (1998), 6108–6114.
- [29] X. Q. Zhu, Y. C. Liu, J. P. Cheng, Which Hydrogen Atom Is First Transferred in the NAD(P)H Model Hantzsch Ester Mediated Reactions via One-step and Multistep hydride transfer?, *J. Org. Chem.* 64, (1999), 8980–8981.
- [30] E. C. Ashby, F. R. Dobbs, H. P. Hopkins, Composition of Lithium Aluminum Hydride, Lithium Borohydride, and Their Alkoxy Derivatives in Ether Solvents as Determined by Molecular Association and Conductance Studies, *J. Am. Chem. Soc.* 97, (1975), 3158–3162.
- [31] E. C. Ashby, J. R. Boone, Mechanism of lithium aluminum hydride reduction of ketones. Kinetics of reduction of mesityl phenyl ketone, *J. Am. Chem. Soc.* 98, (1976), 5524–5531.
- [32] R. T. Luibrand, I. R. Taigounov, A. A. Taigounov, A Theoretical Study of the Reaction of Lithium Aluminum Hydride with Formaldehyde and Cyclohexanone, *J. Org. Chem.* 66, (2001), 7254–7262.
- [33] D. E. Bikiel, F. D. Salvo, M. C. G. Lebrero, F. Doctorovich, D. A. Estrin, Solvation and Structure of LiAlH₄ in Ethereal Solvents, *Inorg. Chem.* 44, (2005), 5286–5292.
- [34] D. C. Wigfield, STEREOCHEMISTRY AND MECHANISM OF KETONE REDUCTIONS BY HYDRIDE REAGENTS, *Tetrahedron* 35, (1979), 449-462.
- [35] R. Bonaccorsi, P. Palla, J. Tomasi, THE MECHANISM OF CARBONYL REDUCTION BY LiBH₄: AN AB INITIO INVESTIGATION, *J. Mol. Struct., Theochem* 87, (1982), 181–196.
- [36] R. Bonaccorsi, R. Clmiraglia, J. Tomasi, S. Miertuš, THE MECHANISM OF CARBONYL REDUCTION BY LiBH₄: AN AB INITIO INVESTIGATION WITH INCLUSION OF SOLVENT EFFECTS, *J. Mol. Struct., Theochem* 94, (1983), 11–23.
- [37] M. J. S. Dewar, M. L. McKee, Ground state of molecules. 50. MNDO study of hydroboration and borohydride reduction. Implications concerning cyclic conjugation and pericyclic reactions, *J. Am. Chem. Soc.* 100, (1978), 7499–7505.
- [38] Y. Suzuki, D. Kaneno, S. Tomoda, Theoretical Study on the Mechanism and Diastereoselectivity of NaBH₄ reduction, *J. Phys. Chem. A* 113, (2009), 2578–2583.

- [39] H. Yamataka, T. Hanafusa, Kinetic Isotope Effect Study of Reductions of Benzophenone with Complex Metal Hydrides, *J. Am. Chem. Soc.* 108, (1986), 6643–6646.
- [40] M. J. Frisch, G. W. Trucks, H. B. Schlegel, G. E. Scuseria, M. A. Robb, J. R. Cheeseman, G. Scalmani, V. Barone, B. Mennucci, G. A. Petersson, H. Nakatsuji, M. Caricato, X. Li, H. P. Hratchian, A. F. Izmaylov, J. Bloino, G. Zheng, J. L. Sonnenberg, M. Hada, M. Ehara, K. Toyota, R. Fukuda, J. Hasegawa, M. Ishida, T. Nakajima, Y. Honda, O. Kitao, H. Nakai, T. Vreven, J. A. Montgomery, Jr., J. E. Peralta, F. Ogliaro, M. Bearpark, J. J. Heyd, E. Brothers, K. N. Kudin, V. N. Staroverov, R. Kobayashi, J. Normand, K. Raghavachari, A. Rendell, J. C. Burant, S. S. Iyengar, J. Tomasi, M. Cossi, N. Rega, J. M. Millam, M. Klene, J. E. Knox, J. B. Cross, V. Bakken, C. Adamo, J. Jaramillo, R. Gomperts, R. E. Stratmann, O. Yazyev, A. J. Austin, R. Cammi, C. Pomelli, J. W. Ochterski, R. L. Martin, K. Morokuma, V. G. Zakrzewski, G. A. Voth, P. Salvador, J. J. Dannenberg, S. Dapprich, A. D. Daniels, Ö. Farkas, J. B. Foresman, J. V. Ortiz, J. Cioslowski, and D. J. Fox, Gaussian, Inc., Wallingford, CT, (2009).
- [41] R. Kobayashi, R. D. Amos, The application of CAM-B3LYP to the charge-transfer band problem of the zincbacteriochlorin-bacteriochlorin complex, *Chem. Phys. Lett.* 420, (2006), 106–109.
- [42] P. A. Limacher, K. V. Mikkelsen, H. P. Lüthi, On the accurate calculation of polarizabilities and second hyperpolarizabilities of polyacetylene oligomer chains using the CAM-B3LYP density functional, *J. Chem. Phys.* 130, (2009), 194114.
- [43] S. Zhang, Z. Qu, P. Tao, B. Brooks, Y. Shao, X. Chen, C. Liu, Quantum Chemical Study of the Ground and Excited State Electronic Structures of Carbazole Oligomers with and without Triarylborane Substitutes, *J. Phys. Chem. C* 116, (2012), 12434-12442.
- [44] Y. Wang, X. Cheng, X. Yang, X. Yang, DFT Study of Solvent Effects for Some Organic Molecules Using a Polarizable Continuum Model, *J. Sol. Chem.* 35, (2006), 869–878.
- [45] M. Najafi, M. Zahedi, E. Klein, DFT/B3LYP study of the solvent effect on the reaction enthalpies of homolytic and heterolytic O-H bond cleavage in mono-substituted chromans, *Comp. Theor. Chem.* 978, (2011), 16–28.
- [46] E. Sigfridsson, U. Ryde, Comparison of methods for deriving atomic charges from the electrostatic potential and moments, *J. Comp. Chem.* 19, (1998), 377–395.
- [47] W. D. Arnold, L. K. Sanders, M. T. McMahon, A. V. Volkov, G. Wu, P. Coppens, S. R. Wilson, N. Godbout, E. Oldfield, Experimental, Hartree-Fock, and Density

Functional Theory Investigations of the Charge Density, Dipole Moment, Electrostatic Potential, and Electric Field Gradients in L-Asparagine Monohydrate, *J. Am. Chem. Soc.* 122, (2000), 4708–4717.

- [48] G. S. Maciel, E. Garcia, Charges derived from electrostatic potentials: Exploring dependence on theory and geometry optimization levels for dipole moments, *Chem. Phys. Lett.* 409, (2005), 29-33.
- [49] F. Martin, H. Zipse, Charge distribution in the water molecule – A comparison of methods, *J. Comp. Chem.* 26, (2005), 97-105.
- [50] K. Hu, L. Wang, X. Liu, Q. Zhuang, Z. Xue, Z. Han, Charge distribution of poly (p-phenylene benzobisoxazole) investigated by quantum chemical simulation, *Comp. Theor. Chem.* 1042, (2014), 1–7.
- [51] G. S. Hammond, A Correlation of Reaction Rates, *J. Am. Chem. Soc.* 77, (1955), 334–338.

Table 1: Activation energy (ΔE_a) and energy difference (ΔE) between reactant and product states for hydride transfer in the vacuum state.

Hydride reagent	ΔE_a (kJ/mol)	ΔE (kJ/mol)
AlH_4^-	49.9	-189
LiAlH_4	10.1	-196
BH_4^-	144.9	-121
LiBH_4	80.8	-117

Table 2: Calculated Bond Lengths (\AA), Angles (deg), Dihedral angles (deg) with hydride transfer of TS, and activation energy ΔE_a , and energy difference ΔE in Explicit model and PCM for LiAlH_4 system.

		Explicit model	PCM
Length (\AA)	Al-H	1.67	1.66
	C-H	1.82	1.79
Angle (deg)	Al-H-C	118	133
Dihedral angle (deg)	Al-H-C-O	25	4
ΔE_a (kJ/mol)		6.51	2.37
ΔE (kJ/mol)		-199	-224

Table 3: Total energies of the RS,^a TS and PS and activation energy (ΔE_a) and energy difference (ΔE) between the RS and PS for hydride transfer.

Hydride reagent	Solvent	E (a.u.)			ΔE_a (kJ/mol)	ΔE (kJ/mol)
		RS	TS	PS		
LiAlH_4	Vacuum	-366.88584	-366.88201	-366.96052	10.1	-196
	THF ($\epsilon^b=7.58$)	-366.91245	-366.91155	-366.99774	2.37	-224
LiBH_4	Vacuum	-149.29184	-149.26107	-149.33650	80.8	-117
	THF ($\epsilon=7.58$)	-149.30878	-149.29741	-149.37483	30.0	-173

^aRS = reactant state, TS = transition state and PS = product state.

^bDielectric constant of the solvent.

Scheme 1. The generally supported hydride reduction mechanism.

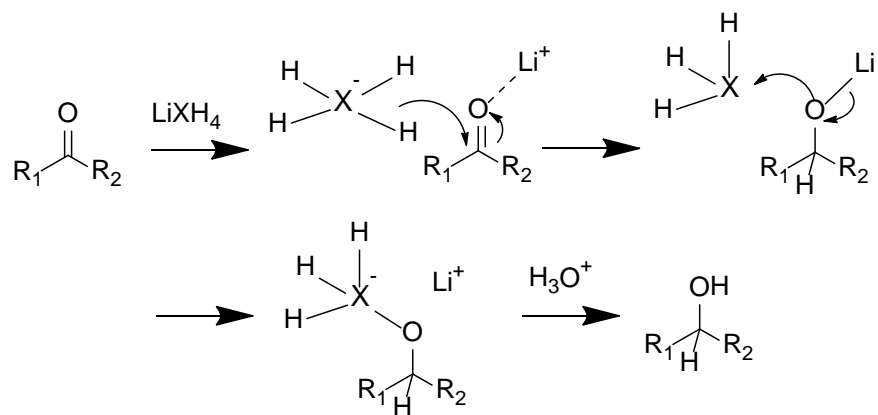


Figure 1. Reactant, transition and product state structures for hydride transfer of (a) LiAlH_4 - and (b) LiBH_4 -formaldehyde complexes in the vacuum state.

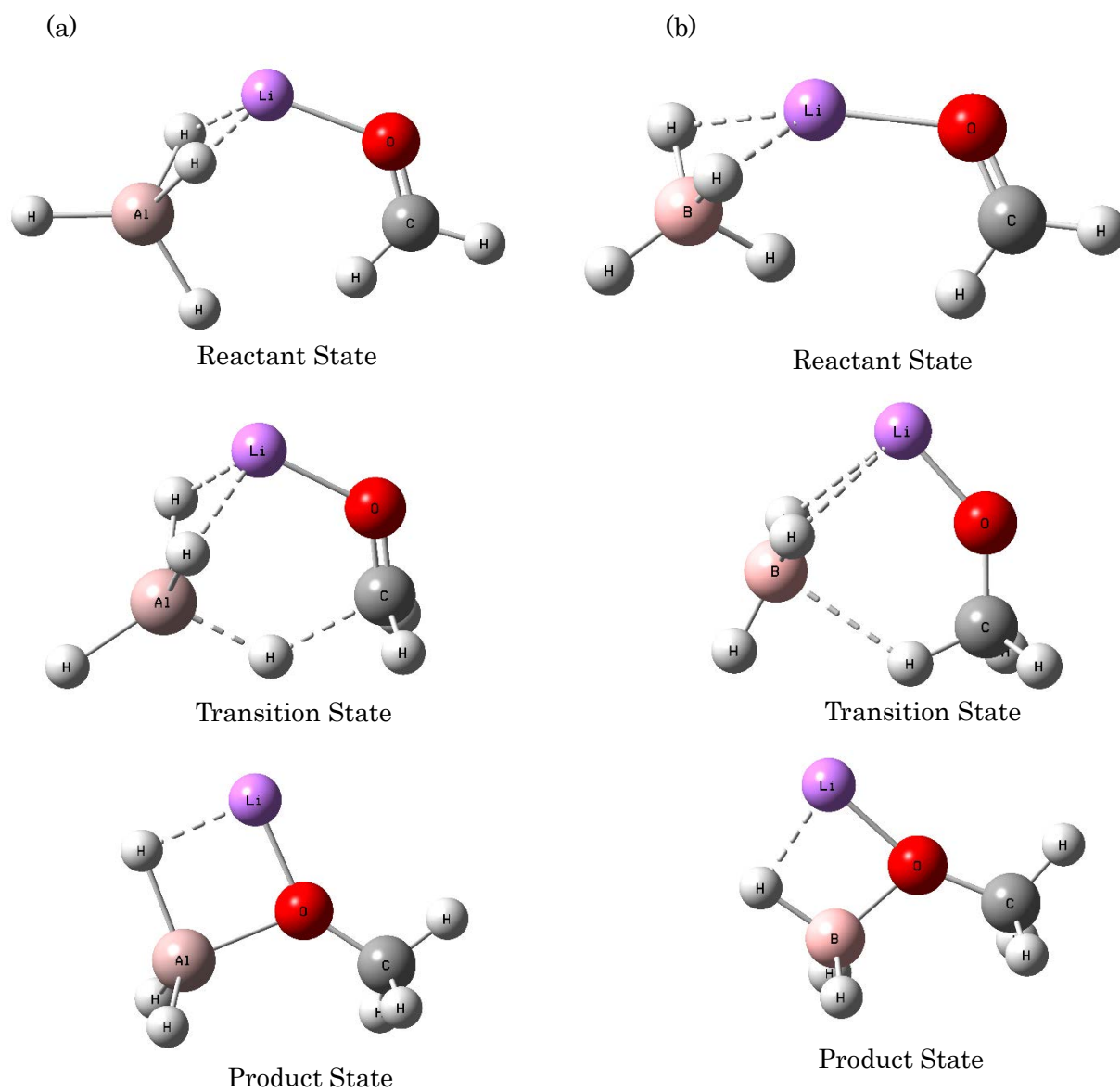


Figure 2. Reactant, transition and product state structures for hydride transfer of LiAlH_4 -formaldehyde complexes including one explicit THF molecule. (This calculation is carried out using Aug-cc-pVDZ basis set.)

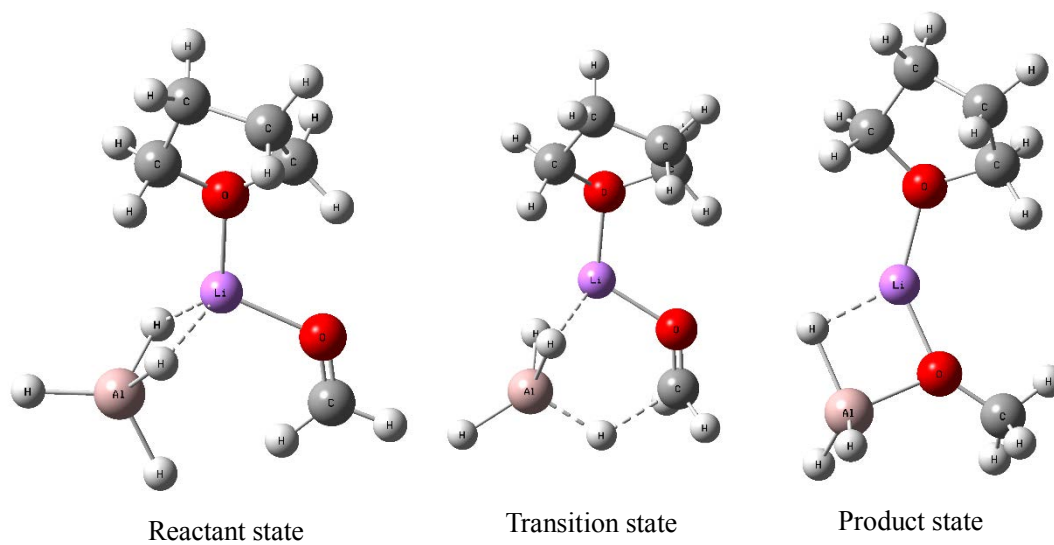


Figure 3. Reactant, transition and product state structures for hydride transfer of (a) LiAlH_4 - and (b) LiBH_4 -formaldehyde complexes in THF.

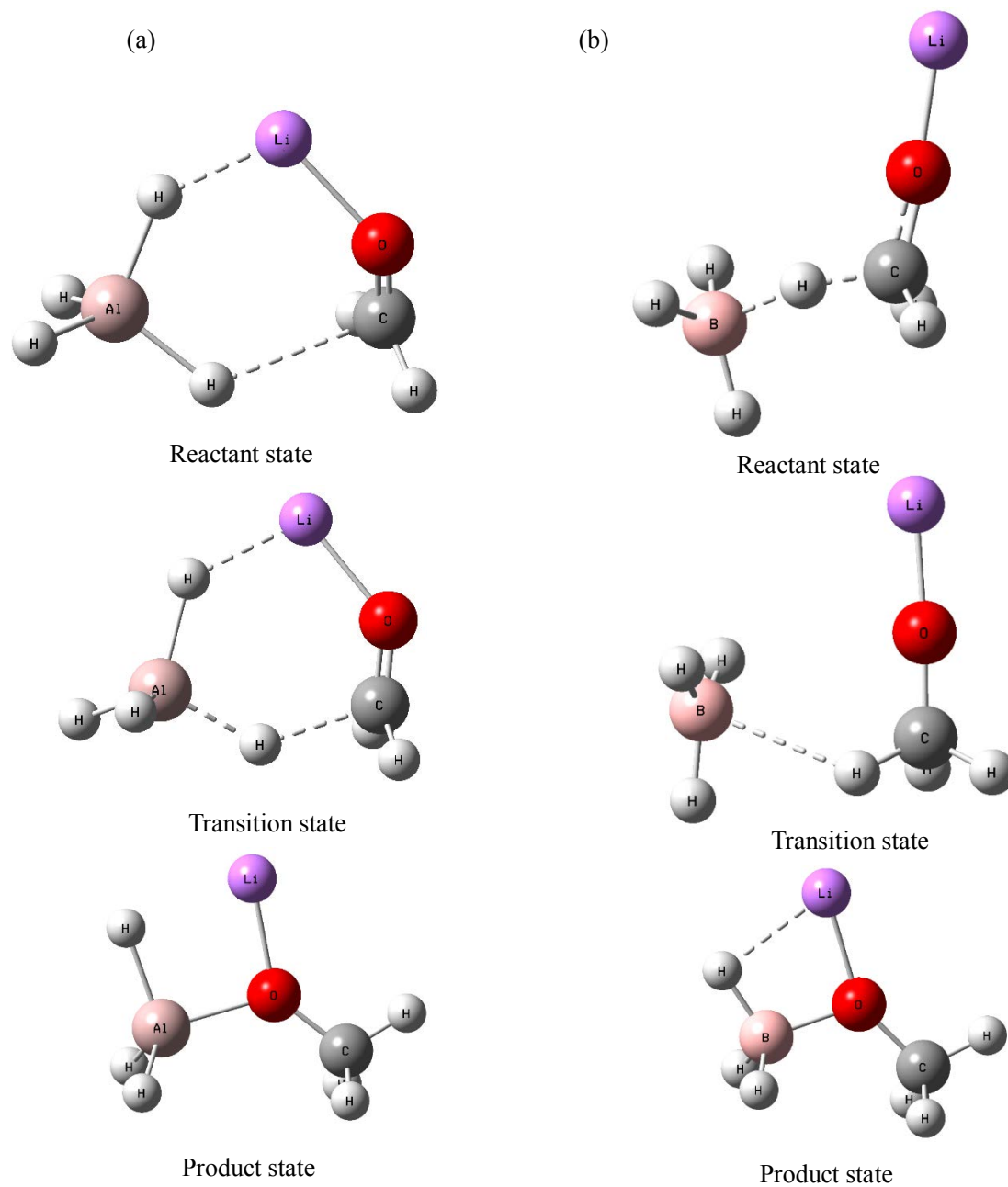


Figure 4. Rearrangement parameter values (blue) and relative energies (red) for the RS along the IRC for the (a) LiAlH_4^- and (b) LiBH_4^- -formaldehyde complexes in the vacuum state.

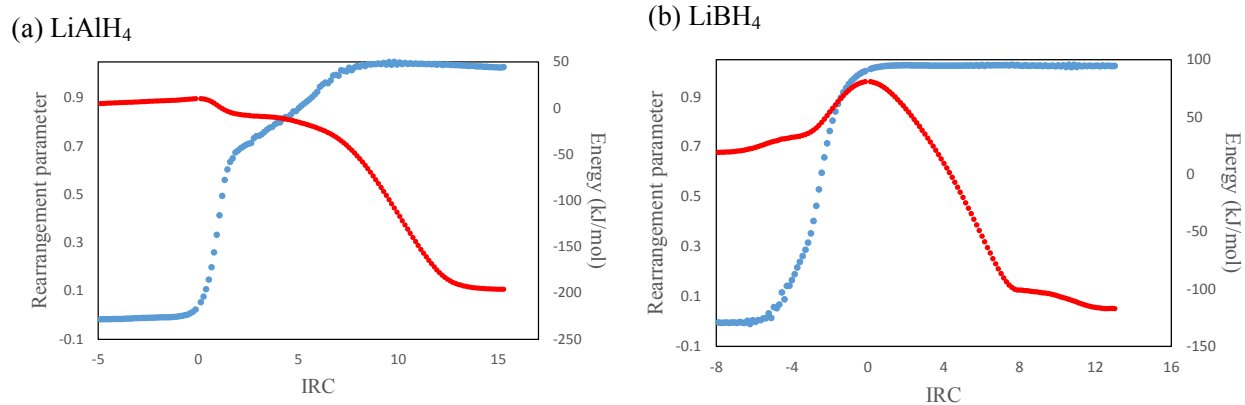


Figure 5. Rearrangement parameter values (blue) and relative energies (red) for the RS along the IRC for the (a) LiAlH_4 - and (b) LiBH_4 -formaldehyde complexes in THF.

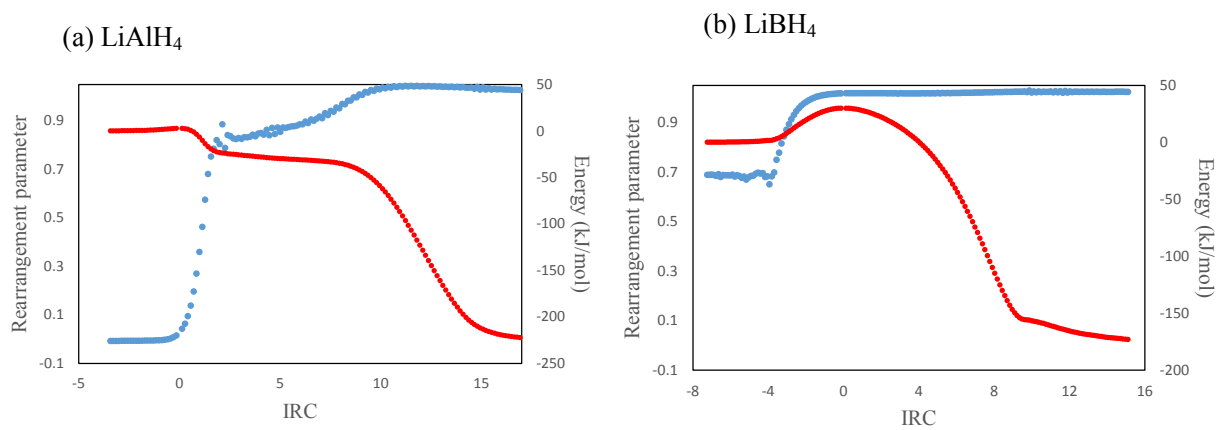


Figure 6. Charge densities of CH₂O (blue), AlH₃ (red) and H (purple) and energy values (black) along the IRC for the (a) LiAlH₄- and (b) LiBH₄-formaldehyde complexes under vacuum.

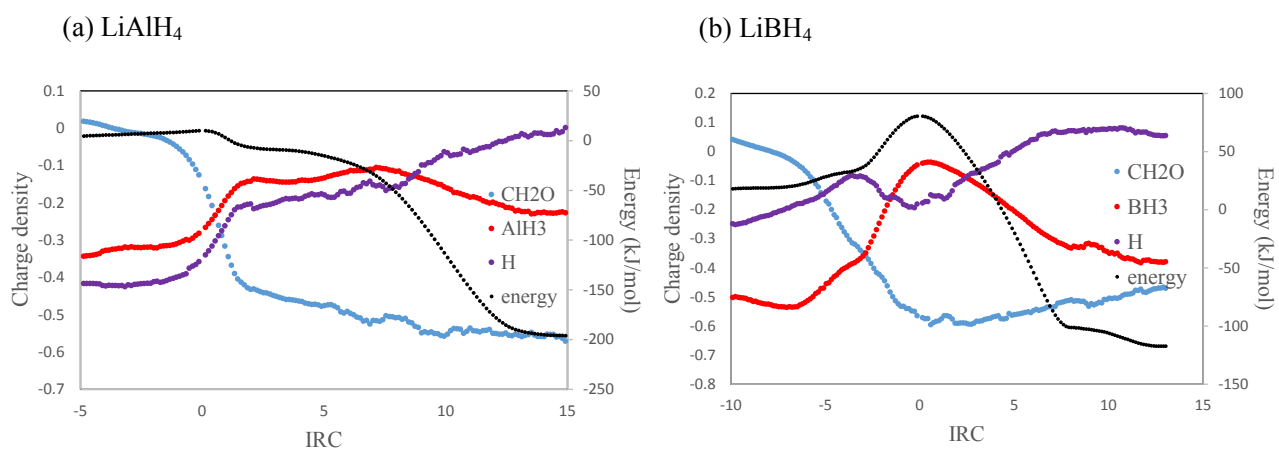


Figure 7. Charge densities of CH₂O (blue), BH₃ (red) and H (purple) and energy values (black) along the IRC for the (a) LiAlH₄- and (b) LiBH₄-formaldehyde complexes in THF.

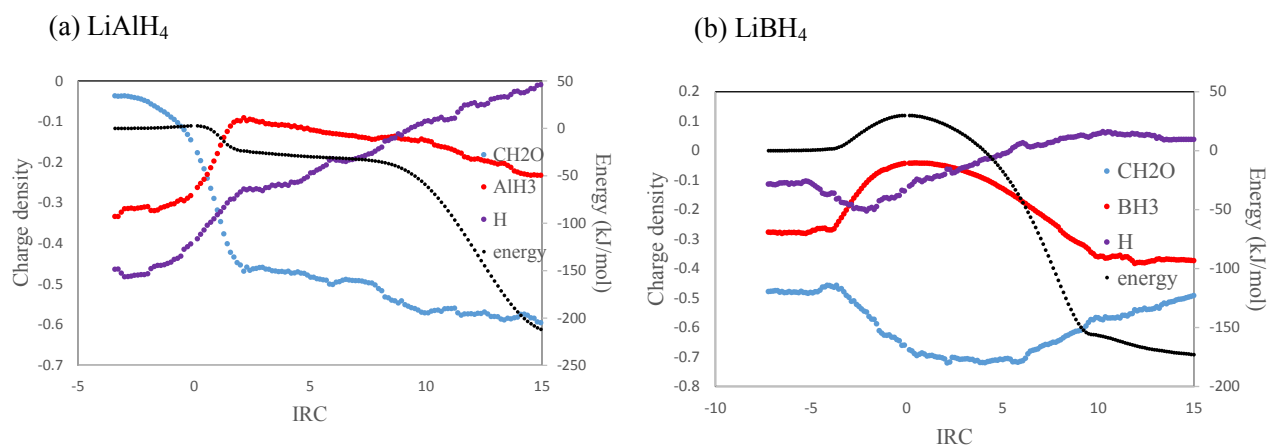
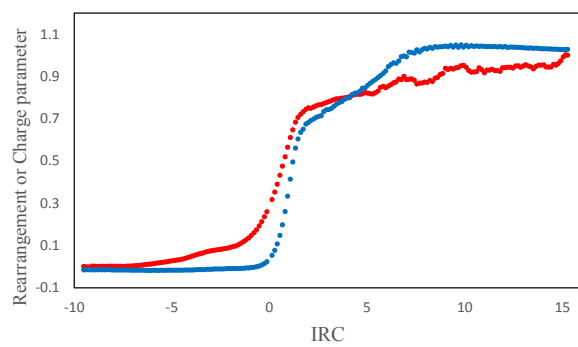


Figure 8. Rearrangement (blue) and charge transfer parameters (red) for (a) LiAlH_4 and (b) LiBH_4 under vacuum.

(a) LiAlH_4



(b) LiBH_4

